PAPER • **OPEN ACCESS**

Phase transitions of alkaline-earth metal sulfides under pressure

To cite this article: Yuefeng Wang *et al* 2021 *Mater. Res. Express* **8** 065902

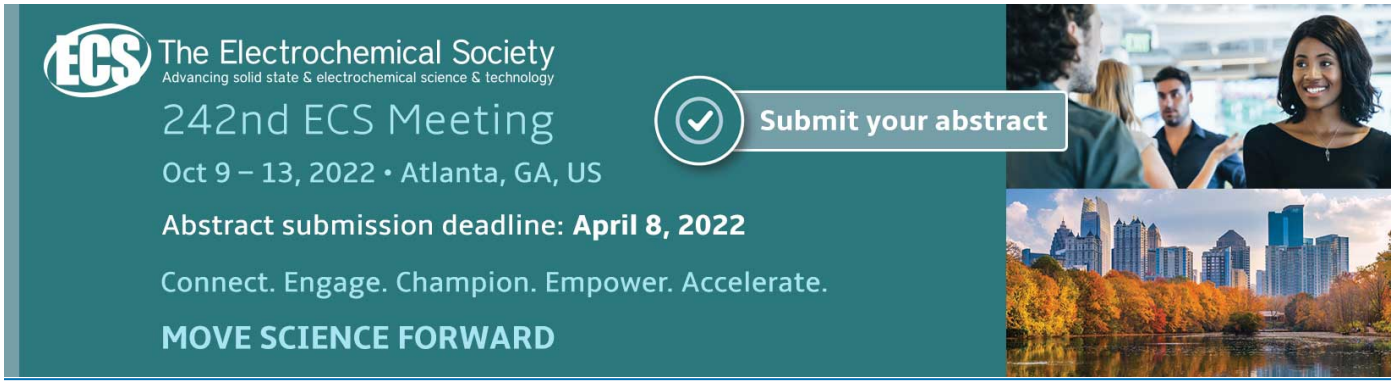

Materials Research Express

OPEN ACCESS

RECEIVED
19 May 2021

REVISED
8 June 2021

ACCEPTED FOR PUBLICATION
10 June 2021

PUBLISHED
21 June 2021

PAPER

Phase transitions of alkaline-earth metal sulfides under pressure

Yuefeng Wang[1], Aitor Bergara[2,3,4], Cancan Shao[1], Lin Wang[1], Xiaowei Liang[1], Linyan Wang[1], Rongxin Sun[1], Xudong Wei[1], Tiansheng Wang[1,5], Guoying Gao[1] and Yongjun Tian[1]

[1] State Key Laboratory of Metastable Materials Science and Technology, Yanshan University, Qinhuangdao 066004, People's Republic of China
[2] Departmento de Física, Universidad del País Vasco, UPV/EHU, 48080 Bilbao, Spain
[3] Donostia International Physics Center (DIPC), 20018 Donostia, Spain
[4] Centro de Física de Materiales CFM, Centro Mixto CSIC-UPV/EHU, 20018 Donostia, Spain
[5] National Engineering Research Center for Equipment and Technology of Cold Strip Rolling, Yanshan University, Qinhuangdao 066004, People's Republic of China

E-mail: gaoguoying@ysu.edu.cn

Keywords: alkaline-earth metal sulfides, structure searching, ab initio calculation, phase transition sequence, modulated structure

Abstract

We have systematically explored the crystal structures of alkaline-earth metal sulfides under pressure by using a swarm-intelligence structural prediction method. At low pressures we successfully reproduced their known structures and phase transition sequences. Under high pressure, MgS is predicted to transform from B28 to a β-NbP-type structure at 262 GPa. CaS and SrS present the same phase transition sequence, from B2 to a β-NbP-type structure, while BaS is predicted to transform to a *Imma* structure. The *Imma* structure is actually similar to the β-NbP-type structure, as it can be seen as a modulated distortion of the latter structure. The absence of any imaginary phonon mode for the predicted structures suggests that they are dynamically stable. The calculated electronic band structures and density of states reveal that all the predicted phases are metallic, except that MgS is a semiconductor. Subsequent electron-phonon coupling calculations suggest that *Imma* BaS is a superconductor with a low T_c of 1.32 K, while β-NbP MgS, CaS and SrS are not superconductors. The current study provides a comprehensive analysis of phase transitions for alkaline-earth metal sulfides up to 300 GPa and might stimulate experimental studies in the future.

1. Introduction

The alkaline-earth metal sulfides *X*S (X = Be, Mg, Ca, Sr, Ba) have recently attracted interest in science and technology because of their remarkable physical properties and wide applications, ranging from catalysis to microelectronics [1–3]. For example, due to their wide semiconducting band gaps, they can be used as excellent host materials to incorporate different impurities (e.g. rare earth ions, transition metal ions) for optical applications, such as multicolor thin film electroluminescent devices, thermoluminescence dosimetry, and cathode ray tubes [4–8]. Pressure is a powerful thermal dynamic parameter which is often used to manipulate the band gap and properties of semiconductors without doping [9–11].

The high-pressure behavior of alkaline-earth metal sulfides have been studied by many theoretical and experimental groups. Under ambient conditions, almost all alkaline-earth metal sulfides crystallize in the rock-salt (B1) structure, with sixfold coordination, except BeS, which presents a fourfold coordinated zinc-blende (B3) structure. At 51 GPa, BeS transforms to a NiAs-type (B8) structure and, then, at 196 GPa a further transition to an orthorhombic structure was predicted by Feng *et al* [12] using a swarm intelligence algorithm. MgS was experimentally observed to be stable in the B1 structure up to 54 GPa [13]. At higher pressures, some groups predicted a CsCl-type (B2) structure at 158–255.5 GPa [14–18], while Wu *et al* [19] suggested a FeSi-type (B28, space group $P2_13$) structure from 143 GPa to 350 GPa. On the other hand, CaS, SrS, and BaS were all observed to transform to the B2 structure at 40, 18, and 6.5 GPa, respectively [20–22].

However, there is not yet complete analysis of MgS, CaS, SrS, and BaS phase transitions up to 300 GPa, which we explore in this article. We predict two new high-pressure structures and complete the phase transition sequence for alkaline-earth metal sulfides below 300 GPa. MgS is predicted to transform from B28 to a β-NbP-type structure, CaS and SrS from B2 to a β-NbP-type structure, while BaS is predicted to transform to a *Imma* structure.

2. Computational details

Structure searches of XS (X = Mg, Ca, Sr, Ba) were performed at 1 atm, 10, 50, 100, 150, 200, 250, and 300 GPa, using the recently developed CALYPSO code, which requires only chemical compositions for the given compounds [23–29]. The maximum formula units (f.u.) considered per simulation cell at each pressure is eight. Based on density functional theory, structural optimizations were performed using the generalized gradient approximation [30] (within Perdew–Burke–Ernzerhof parametrization), as implemented in the Vienna *ab initio* simulation package [31]. The all-electron projector augmented-wave method [32] was used to describe the electron-ion interaction. For Mg, Ca, Sr, Ba and S, $3s^2$, $3s^23p^64s^2$, $4s^24p^65s^2$, $5s^25p^66s^2$ and $3s^23p^4$ configurations are considered as valence electrons, respectively. A kinetic energy cutoff of 600 eV and appropriate Monkhorst–Pack [33] k meshes were chosen to ensure enthalpy convergence within 1 meV/f.u. A supercell approach [34] was used to calculate the phonon spectra with the PHONOPY code [35]. Electron-phonon coupling (EPC) calculations were done through the widely used Quantum-ESPRESSO code [36]. Ultrasoft pseudopotentials were employed and convergence tests gave a kinetic energy cutoff of 60 Ry. $7 \times 7 \times 7$ and $6 \times 6 \times 6$ q-point meshes in the first Brillouin zone were used for β-NbP MgS, CaS, SrS and *Imma* BaS, respectively. Correspondingly, $28 \times 28 \times 28$ and $24 \times 24 \times 24$ Monkhorst-Pack grids were used to ensure k-point sampling convergence with Gaussians of width 0.02 Ry, respectively, which approximates the zero-width limit for calculating the EPC parameter λ. λ can be defined as the first reciprocal moment of the spectral function $\alpha^2F(\omega)$,

$$\lambda = 2\int_0^\infty \frac{\alpha^2F(\omega)}{\omega}d\omega \approx \sum_{qj}\lambda_{qj}\omega(q), \tag{1}$$

where $w(q)$ is the weight of a q point in the first Brillouin zone, and $\alpha^2F(\omega)$ is expressed by the phonon linewidth γ_{qj}, owing to electron-phonon coupling [37–39]:

$$\alpha^2F(\omega) = \frac{1}{2\pi N_f}\sum_{qj}\frac{\gamma_{qj}}{\omega_{qj}}\delta(\omega - \omega_{qj})\omega(q), \tag{2}$$

where N_f is the electronic density of states at the Fermi level. The linewidth γ_{qj} of a phonon mode j at wave vector q, arising from EPC is given by

$$\gamma_{qj} = 2\pi\omega_{qj}\sum_{knm}|g^j_{kn,k+qm}|^2\delta(\varepsilon_{kn})\delta(\varepsilon_{k+qm}), \tag{3}$$

where the sum is over the Brillouin zone, and ε_{kn} are the energies of bands measured with respect to the Fermi level at point k, and $g^j_{kn,k+qm}$ is the electron-phonon matrix element. The critical temperature T_c has been estimated from the Allen-Dynes modified McMillan equation [40]:

$$T_C = \frac{\omega_{\log}}{1.2}\exp\left[-\frac{1.04(1+\lambda)}{\lambda - \mu^*(1+0.62\lambda)}\right], \tag{4}$$

Where $\mu*$ is the Coulomb pseudopotential, and $\omega_{\log}$ is the logarithmic average of the phonon frequencies and can be expressed as

$$\omega_{\log} = \omega_0\exp\left[\frac{2}{\lambda}\int\frac{\alpha^2F(\omega)}{\omega}\log\frac{\omega}{\omega_0}d\omega\right]. \tag{5}$$

3. Results and discussion

At ambient pressure, MgS, CaS, SrS, and BaS are all predicted to be stable in the B1 structure, which is in good agreement with the experimental results [13, 20–22]. The calculated lattice parameters, elastic constants and formation energies of the predicted B1 MgS, CaS, SrS, and BaS together with experimental or previously theoretical results are shown in table 1, which are in good agreement with each other. For MgS, the B28 and β-NbP-type structures (space group $I4_1/amd$) with the lowest enthalpies are predicted at 150–200 and 300 GPa,

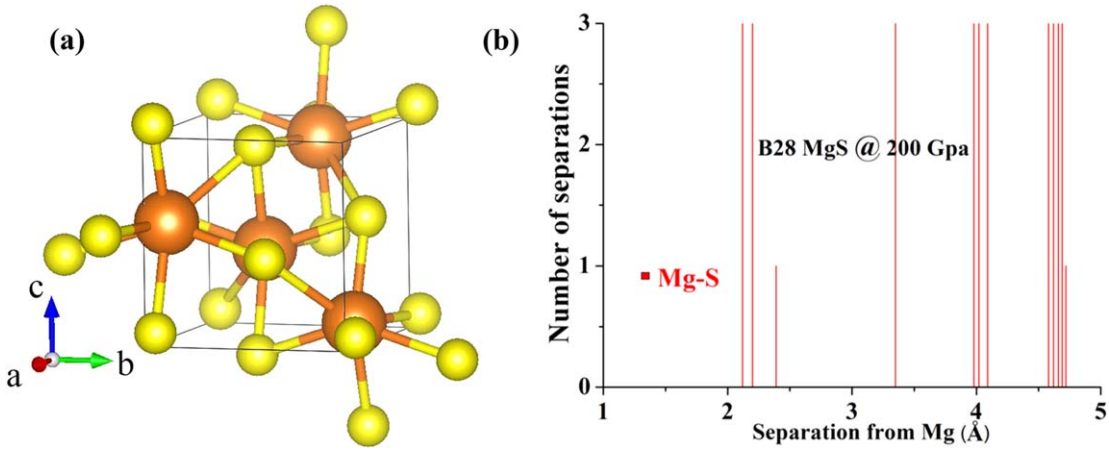

Figure 1. (a) and (b) are the predicted B28 structure and the corresponding histogram of Mg-S separations for MgS at 200 GPa, respectively. Mg's are depicted as large orange spheres and S's as small yellow ones.

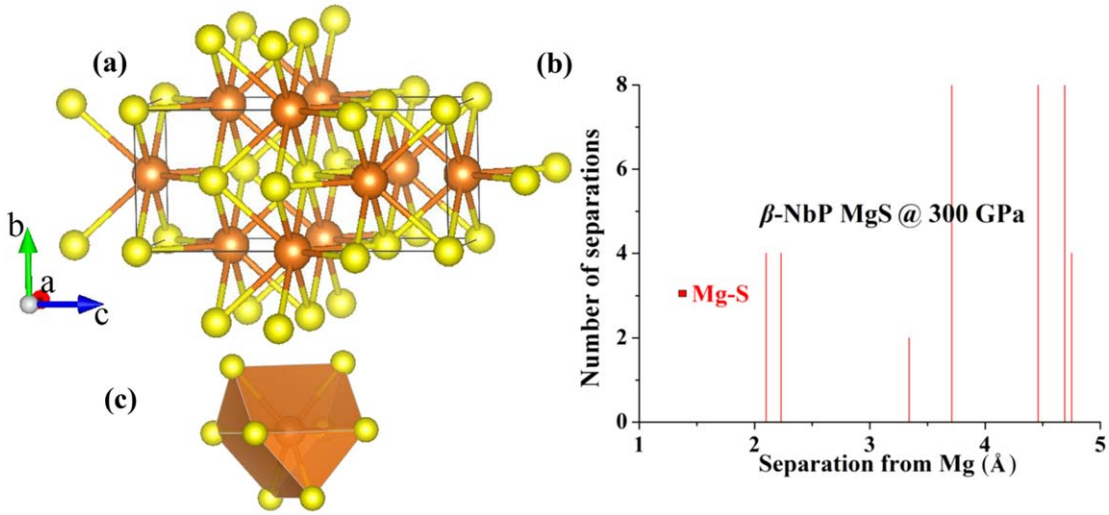

Figure 2. (a) and (b) are the predicted β-NbP-type structure and the corresponding histogram of Mg–S separations for MgS at 300 GPa, respectively. (c) One octahedron unit. Mg's are depicted as large orange spheres and S's as small yellow ones.

Table 1. The calculated lattice parameters (Å), elastic constants (C11, C12, and C44, GPa) and formation energies (eV/atom) of the predicted B1 MgS, CaS, SrS, and BaS are compared with experimental or previously theoretical results.

Compounds		a	*C*11	*C*12	*C*44	E_{form}
B1 MgS	Present	5.21	137.9	42.8	51.1	−1.45
	Others [41, 42]	5.19	140	42	54	−1.68
B1 CaS	Present	5.72	123.3	23.7	33	−2.17
	Others [41, 42]	5.68	123	24	33	−2.40
B1 SrS	Present	6.06	107.8	18.9	25.8	−2.16
	Others [41, 42]	6.01	106	17	26	−2.40
B1 BaS	Present	6.45	90.2	16.9	18.7	−2.09
	Others [42, 43]	6.37	91	17	19	−2.33

respectively. For CaS, and SrS, the B2 and the β-NbP-type structures are predicted at 50–150 and 200–300 GPa, respectively. The B2 structure is also predicted at 10–250 GPa for BaS, while a *Imma* structure at higher pressure.

The B28 structure (group space $P2_13$, FeSi-type) for MgS, which is shown in figure 1(a), is a primitive-cubic structure with 8 atoms unit^{-1} cell. This structure is very simple and high-symmetry but with an unusual sevenfold coordination (see figure 1(b)) of both the Mg and S atoms. Each Mg atom is surrounded by seven S

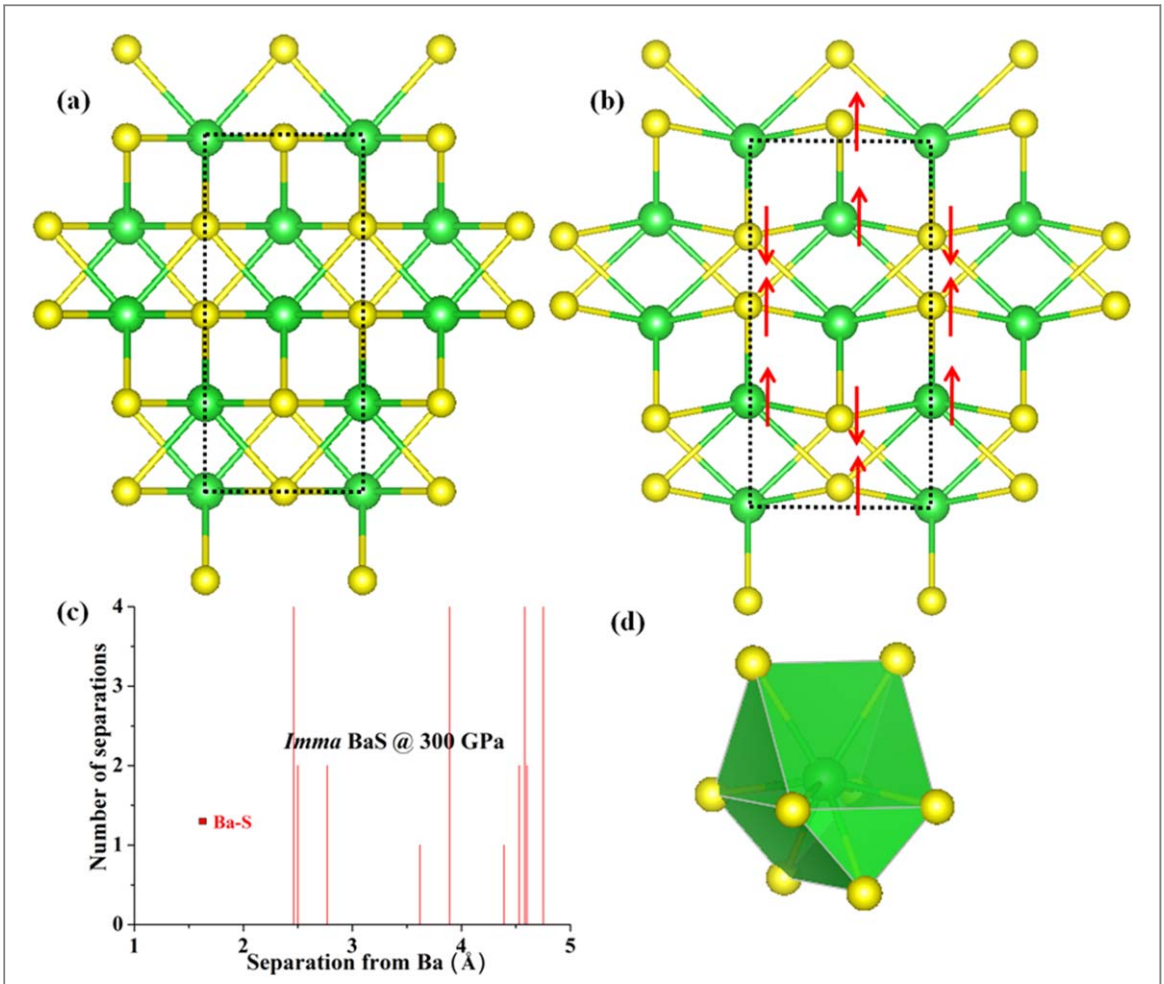

Figure 3. (a) Predicted β-NbP-type structure for BaS at 100 GPa and its conventional unit cell is indicated by a dashed line. (b) and (c) are the predicted *Imma* structure and the corresponding histogram of Ba–S distances for BaS at 300 GPa, respectively. The displacements of Ba atoms and S atoms in the *Imma* structure relative to that in the β-NbP-type structure are parallel or anti-parallel with respect to the *Z* axis in the *XZ* plane indicated by arrows in (b). (d) One octahedron unit. Ba's are depicted as large green spheres and S's as small yellow ones.

atoms, and each S atom by seven Mg atoms, at distances of 2.38 Å, 2.12 (×3) Å, 2.20 (×3) Å of 200 GPa. In addition, each Mg atom has six next nearest Mg atoms with the same distance of 2.55 Å, whereas each S atom has six next nearest S atoms with 2.57 Å at 200 GPa.

The β-NbP-type structure belongs to a tetragonal crystal system with 8 atoms unit^{-1} cell, as is shown in figure 2(a). In this structure, Mg and S form face-centered tetragonal sublattices, and the histogram of Mg–S separation is shown in figure 2(b). This histogram shows a clear gap between the shortest Mg–S distances of 2.1–2.23 Å, and the longer separations of 3.34–3.71 Å. According to this gap, we can easily conclude that the coordination number for β-NbP MgS is eight. In addition, each Mg atom is close to eight S atoms forming an octahedron which is composed of square-face-sharing two triangular prisms, where the Mg atom locates at the center of the square-face (figure 2(c)), and vice versa. The predicted *Imma* structure for BaS is a body-centered orthorhombic structure with 8 atoms unit^{-1} cell and it can be seen as a modulated distortion of the β-NbP-type structure. The modulated distortion occurs with the change of atomic displacement in the *XY* plane, specifically, it is enlarging along the *X* axis and compressing along the *Y* axis. These distortions cause highly distorted face-centered orthorhombic sublattices formed by Ba and S in the modulated structure, in which all S atoms and partial face-centered Ba atoms are displaced along the *Z* axis (figures 3(a) and (b)). According to the histogram of Ba–S separations in *Imma* BaS (figure 3(c)), we can conclude that the coordination number for *Imma* BaS is also eight. Each Ba atom is also coordinated with eight S atoms forming an octahedron which is composed of face-sharing two different triangular prisms, but Ba atom is not located on the face (figure 3(d)). Although pressure-induced modulated structures are not so common in simple binary compounds [12], this study provides such an example.

Enthalpy calculations as a function of pressure for MgS, CaS, SrS and BaS are presented in figure 4. MgS is stable in the B1 structure below 140 GPa, above which the B28 structure becomes stable (figure 4(a) and its inset). At 262 GPa, a predicted β-NbP-type structure is then preferred. Figures 4(b)–(d) show that CaS, SrS, and

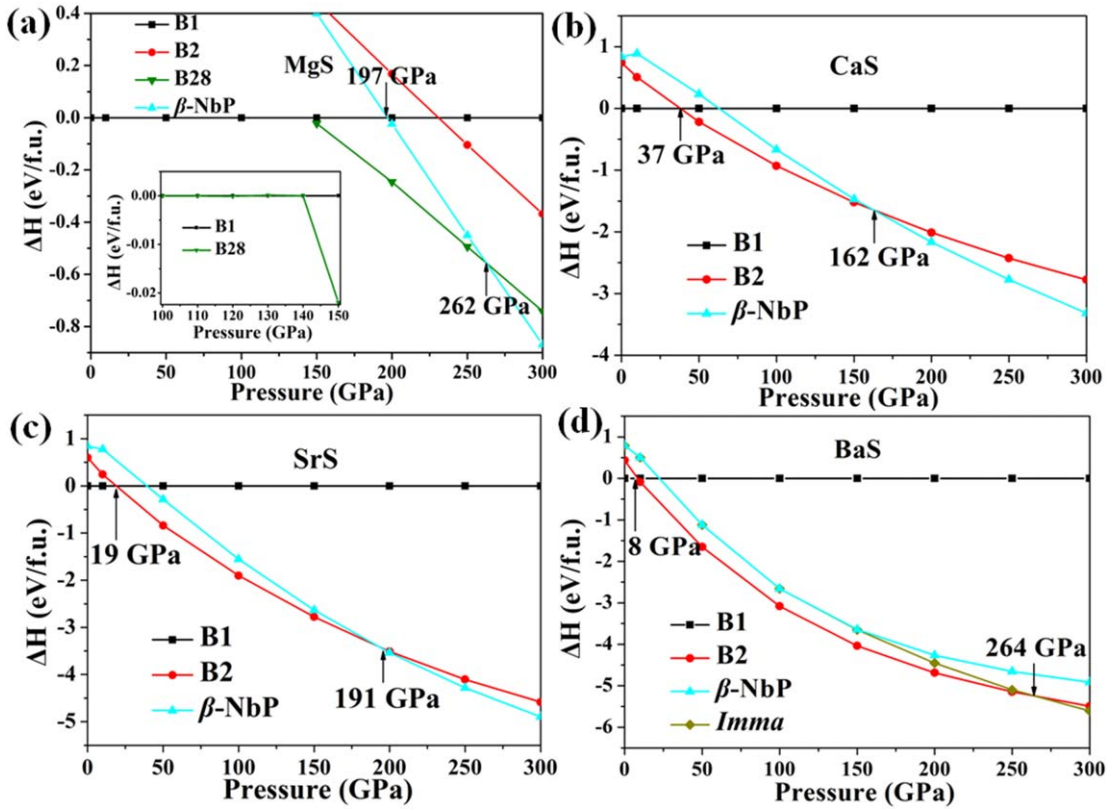

Figure 4. Ground-state static enthalpy curves per f.u. for (a) MgS, (b) CaS, (c) SrS, and (d) BaS as a function of pressure, with respect to the B1 structure. The inset in (a) shows that the B28 structure for MgS has a lower enthalpy than the B1 structure above 140 GPa.

Table 2. Lattice parameters of the predicted new structures of alkaline-earth metal sulfides.

Compounds	Pressure (GPa)	Space group	Lattice parameters (Å, degree)	Atomic positions (fractional)
MgS	200	$P2_13$	a = b = c = 4.104,	Mg 0.413 0.413 0.413
		(B28)	$\alpha=\beta=\gamma=90°$	S 0.077 0.077 0.077
	300	$I4_1/amd$	a = b = 2.964, c = 6.673,	Mg 0.500 0.000 0.750
		(β-NbP)	$\alpha=\beta=\gamma=90°$	S 0.500 0.000 0.250
CaS	200	$I4_1/amd$	a = b = 3.314, c = 7.159,	Ca 0.500 0.000 0.750
		(β-NbP)	$\alpha=\beta=\gamma=90°$	S 0.500 0.000 0.250
SrS	200	$I4_1/amd$	a = b = 3.479, c = 7.299,	Sr 0.500 0.000 0.750
		(β-NbP)	$\alpha=\beta=\gamma=90°$	S 0.500 0.000 0.250
BaS	300	*Imma*	a = 4.033, b = 2.728,	Ba 0.000 0.750 0.143
			c = 8.009, $\alpha=\beta=\gamma=90°$	S 0.000 0.750 0.595

BaS have the same B1–B2 phase transition at 37, 19, and 8 GPa, respectively, which is in agreement with the corresponding experimental results of 40, 18, and 6.5 GPa [20–22]. The corresponding differences are 3, 1, and 1.5 GPa, respectively. Above 162 and 191 GPa, CaS and SrS will transform to the same β-NbP-type structure, respectively, while BaS will be stable in the *Imma* structure above 264 GPa. The specific structure information of the predicted structures is shown in table 2.

The complete phase transition sequences of alkaline-earth metal sulfides up to 300 GPa are summarized in figure 5. The phase transition sequence of MgS is B1 → B28→β-NbP under pressure. CaS and SrS present the same phase transition sequence of B1 → B2→β-NbP, while BaS has a different one, B1 → B2 → *Imma*. At low pressures MgS, CaS, and SrS are all stable in the B1 structure and at very high pressures they stabilize in the β-NbP-type structure. The main difference is that CaS and SrS transform into the β-NbP-type structure from the B2 structure, while in MgS it does so from the B28 structure. At low pressures CaS, SrS and BaS have the same phase transition sequence, B1 → B2, while at high pressures it is predicted that CaS and SrS will transform into the β-NbP-type structure and BaS into a *Imma* structure.

Taking into account that the *Imma* structure derives from a modulated distortion of the β-NbP-type structure, the phase transition sequence of BaS can be considered to be similar to that of CaS and SrS. However,

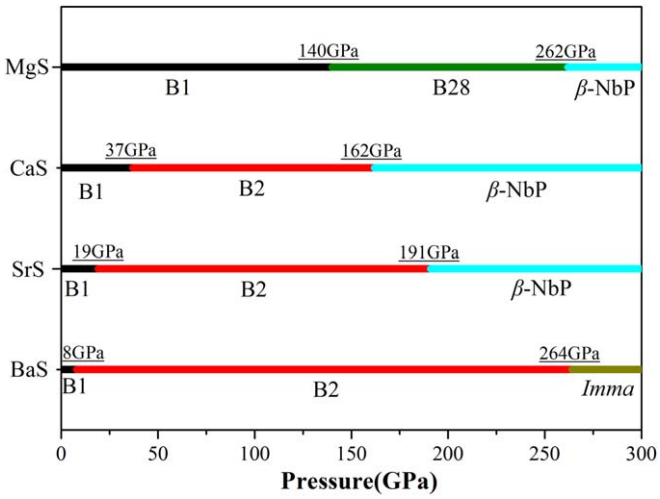

Figure 5. Phase transition sequences for alkaline-earth metal sulfides up to 300 GPa.

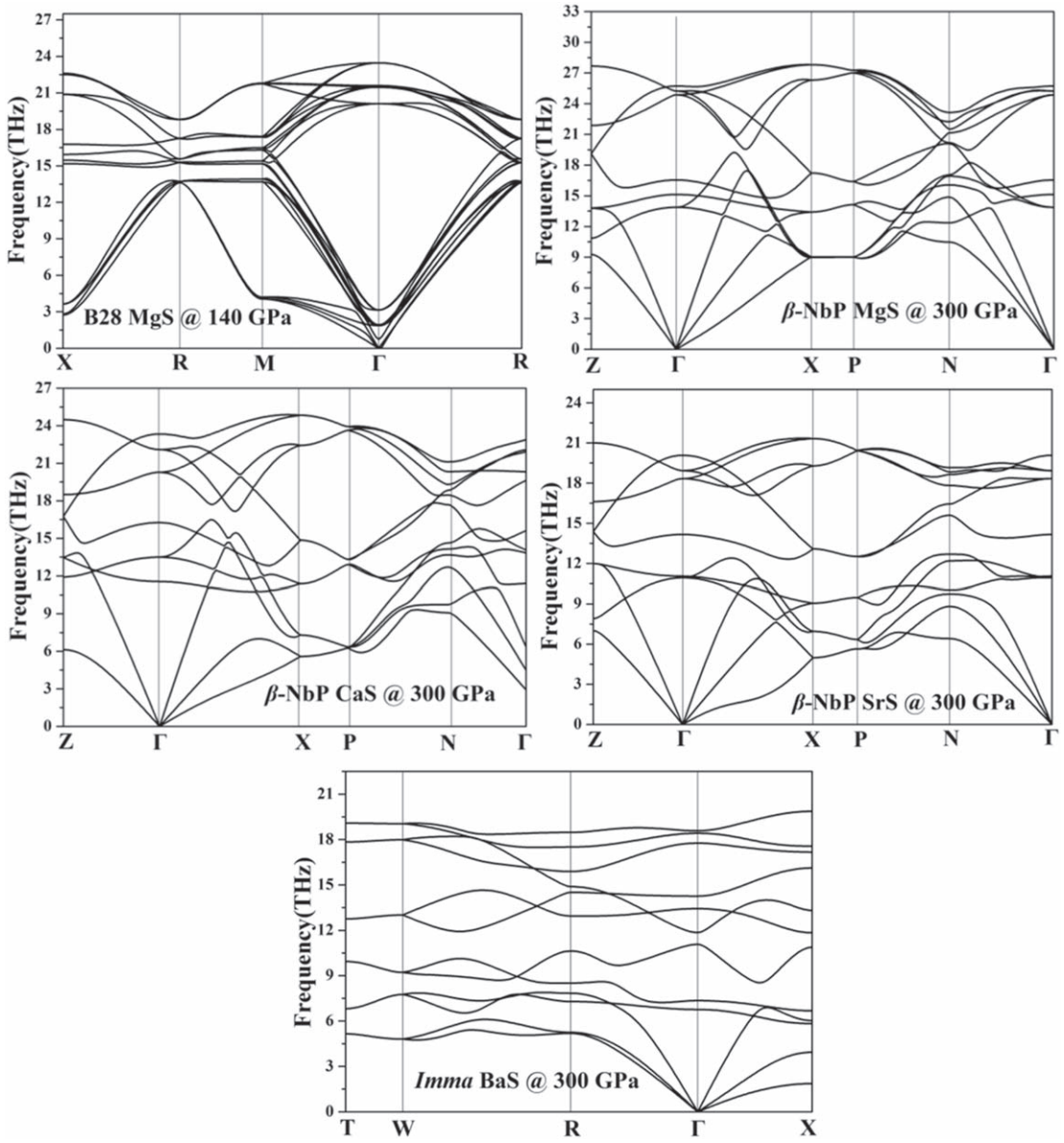

Figure 6. Calculated phonon dispersion curves of the predicted novel structures of the alkaline-earth metal sulfides at pressures corresponding to their thermodynamically stable range.

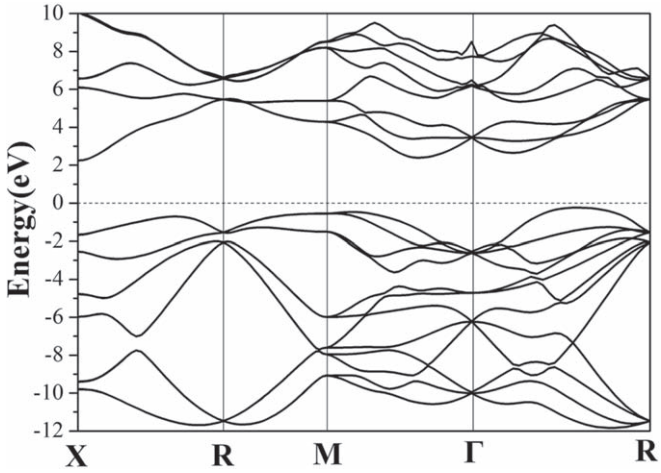

Figure 7. Calculated electronic band structure of B28 MgS at 200 GPa.

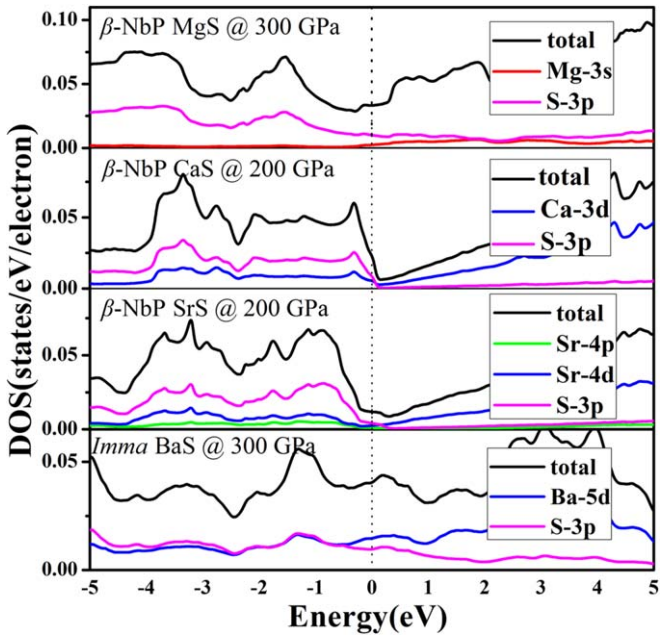

Figure 8. Calculated electronic DOS per valence electron of β-NbP MgS, CaS and SrS, and *Imma* BaS at 300, 200, 200 and 300 GPa, respectively. All these sulfides are metallic.

the phase transition sequence of MgS is different. The reason of this difference can be due to the pressure-induced electronic *s* to *d* mixing observed in Ca, Sr and Ba, but not in Mg. For pure solids at 1atm, the energies of the unoccupied 3*d*, 4*d*, and 5*d* states in Ca, Sr, and Ba, are quite close to the occupied 4*s*, 5 *s*, and 6 *s* states, respectively [1]. Under pressure, the *s* electrons get trapped between the nuclei and they are excluded from them due to the requirement of orthogonality with core electronic states and the decrease of the atomic volume. Thus, under pressure, the *s* band energy rises relative to the *d* band until these *s* electrons start to occupy the *d* band [44]. This *s* to *d* mixing in CaS, SrS, and BaS explains why they present a similar phase transition sequence, which is different from that of MgS, since Mg does not show the above mentioned *s*/*d* mixing.

Analyzing the phase transition sequences of alkaline-earth metal sulfides we can see that the B1–B2 transition pressure of the compounds decreases from CaS, SrS to BaS, while it increases in the B2–β-NbP (or *Imma*) transition sequence. At low pressures, the decrease of the B1–B2 transition pressure for heavier metal atoms is mainly due to the chemical precompression. With increasing pressure, the role of the electrostatic interaction between the ions (Madelung energy) becomes more important and complicated [45]; so that the increase of the B2–β-NbP (or *Imma*) phase transition pressure from CaS, SrS to BaS at high pressures might be due to the enhancement of the Madelung energy with pressure.

Table 3. The calculated EPC parameter λ, phonon frequency logarithmic average ω_{log} and critical temperature T_c ($\mu^* = 0.1$) from the Allen-Dynes modified McMillan equation for β-NbP MgS, CaS and SrS and *Imma* BaS.

Compounds	Pressure (GPa)	λ	ω_{log} (K)	T_c (K) ($\mu^* = 0.1$)
β-NbP MgS	300	0.24	626	0.02
β-NbP CaS	200	0.25	451	0.03
β-NbP SrS	200	0.19	444	0.00
Imma BaS	300	0.37	498	1.32

To explore the dynamical stability of the predicted B28 MgS, β-NbP MgS, CaS and SrS, and *Imma* BaS, we have calculated their phonon dispersion curves at the corresponding stable pressure ranges (figure 6). Due to there are no imaginary frequency in the whole Brillouin zone, these structures are all dynamically stable.

Figures 7 and 8 present the calculated electronic band structure and density of states (DOS) for static B28 MgS, β-NbP MgS, CaS and SrS, and *Imma* BaS at 200, 300, 200, 200 and 300 GPa, respectively. Interestingly, as it is shown in figure 7, at 200 GPa MgS is a semiconductor with an indirect band gap of 2.48 eV (calculated with a HSE hybrid functional [46, 47], which is reasonably reliable to estimate band gaps). However, the other alkali-earth metal sulfides are all metallic (figure 8). An analysis of the contributions of different atomic orbitals to the total electronic DOS indicates that at the Fermi level there is an important contributions from S 3*p* orbitals, while in BaS there are more contributions from Ba 5*d* orbitals.

To investigate the superconductivity of metallic β-NbP MgS, CaS, and SrS and *Imma* BaS, the T_c values of these predicted phases were estimated by using the Allen-Dynes modified McMillan equation [40]. As shown in table 3, the estimated T_c values of β-NbP MgS, CaS and SrS are close to 0 K, and the T_c for *Imma* BaS is 1.32 K with μ^* of 0.1. The weak EPC, small phonon vibration frequencies and low electronic DOS at the Fermi level (figure 8) lead to the very small T_c in these systems.

4. Conclusions

We have systematically studied the phase transitions of the alkaline-earth metal sulfides XS (X = Mg, Ca, Sr, Ba) under pressure. MgS first transforms from B1 to the B28 structure and then to the β-NbP-type structure. At low pressures CaS, SrS and BaS have the same phase transition sequence, B1 $\rightarrow$ B2, while at high pressures it is predicted that CaS and SrS will transform into the β-NbP-type structure and BaS into a *Imma* structure, which is actually a modulated distortion of the β-NbP-type structure. All the predicted phases are dynamically stable and metallic, except MgS which is a semiconductor. Moreover, *Imma* BaS is estimated to be superconducting with a T_c of 1.32 K.

Acknowledgments

The work was supported by National Natural Science Foundation of China (91963115, 52022089), the PhD Foundation by Yanshan University (B970), Science and Technology Project of Hebei Education Department (Grant No. QN2021136). A.B. acknowledges financial support from the Spanish Ministry of Science and Innovation (PID2019-105488GB-I00).

Data availability statement

All data that support the findings of this study are included within the article (and any supplementary files).

ORCID iDs

Guoying Gao https://orcid.org/0000-0003-3823-2942

References

[1] Chakrabarti A 1999 *Phys. Rev. B* **62** 1806–14
[2] Li Y, Ma Y, Cui T, Yan Y and Zou G 2008 *Appl. Phys. Lett.* **92** 101907
[3] Rached D, Rabah M, Benkhettou N, khenata R, Soudini B, Al-Douri Y and Baltache H 2006 *Comput. Mater. Sci.* **37** 292–9
[4] Yamashita N 1984 *J. Phys. Soc. Jpn.* **53** 2400–6

[5] Wang M W, Swenberg J F, Phillips M C, Yu E T and McCaldin J O 1994 *Appl. Phys. Lett.* **64** 3455–7
[6] Pandey R and Sivaraman S 1991 *J. Phys. Chem. Solids* **52** 211–25
[7] Yamashita N and Asano S 1987 *J. Phys. Soc. Jpn.* **56** 352–8
[8] Rao R P 1986 *J. Mater. Sci.* **21** 3357–86
[9] Yuan Y, Li Y, Fang G, Liu G, Pei C, Li X, Zheng H, Yang K and Wang L 2019 *Nat. Sci. Rev.* **6** 524–31
[10] Huang Y *et al* 2019 *Nat. Sci. Rev.* **6** 239–46
[11] Pei C and Wang L 2019 *Matter Radiat. Extremes* **4** 028201
[12] Feng X, Gao P, Li X, Li X, Wu M, Wang H, Lv J, Redfern S A T, Liu H and Ma Y 2019 *Phys. Rev. B* **100** 014102
[13] Peiris S M, Campbell A J and Heinz D L 1994 *J. Phys. Chem. Solids* **55** 413–9
[14] Ekbundit S, Chizmeshya A, Laviolette R and Wolf G H 1996 *J. Phys.: Condens. Matter* **8** 8251–65
[15] Camp P E V, Doren V E V and Martins J L 1995 *Phys. Status Solidi B* **190** 193–7
[16] Jha P, Sakalle U K and Sanyal S P 1998 *J. Phys. Chem. Solids* **59** 599–603
[17] Varshney D, Kaurav N, Sharma U and Singh R K 2008 *J. Phys. Chem. Solids* **69** 60–9
[18] Guo Y D, Yang Z J, Gao Q H and Dai W 2008 *Physica B* **403** 2367–71
[19] Wu H Y, Chen Y H, Su X F, Deng C R and Liu Z J 2014 *Philos. Mag. Lett.* **94** 198–204
[20] Luo H, Greene R G, Ghandehari K, Li T and Ruoff A L 1994 *Phys. Rev. B* **50** 16232–7
[21] Syassen K 1985 *Phys. Status Solidi A* **91** 11–5
[22] Weir S T, Vohra Y K and Ruoff A L 1986 *Phys. Rev. B* **33** 4221–6
[23] Wang Y, Lv J, Zhu L and Ma Y 2010 *Phys. Rev. B* **82** 094116
[24] Wang Y, Lv J, Zhu L and Ma Y 2012 *Comput. Phys. Commun.* **183** 2063–70
[25] Zhu L, Liu H, Pickard C J, Zou G and Ma Y 2014 *Nat. Chem.* **6** 644–8
[26] Lv J, Wang Y, Zhu L and Ma Y 2011 *Phys. Rev. Lett.* **106** 015503
[27] Liang X, Bergara A, Wang L, Wen B, Zhao Z, Zhou X F, He J, Gao G and Tian Y 2019 *Phys. Rev. B* **99** 100505
[28] Wang L *et al* 2019 *Phys. Rev. B* **99** 174104
[29] Wang L *et al* 2020 *Sci. China Mater.* **63** 2358–64
[30] Perdew J P, Burke K and Ernzerhof M 1996 *Phys. Rev. Lett.* **77** 3865–8
[31] Kresse G and Furthmüller J 1996 *Phys. Rev. B* **54** 11169–86
[32] Blochl P E 1994 *Phys. Rev. B* **50** 17953–79
[33] Monkhorst H J and Pack J D 1976 *Phys. Rev. B* **13** 5188–92
[34] Parlinski K, Li Z Q and Kawazoe Y 1997 *Phys. Rev. Lett.* **78** 4063–6
[35] Togo A, Oba F and Tanaka I 2008 *Phys. Rev. B* **78** 134106
[36] Giannozzi P *et al* 2009 *J. Phys.: Condens. Matter* **21** 395502
[37] Allen P B and Silberglitt R 1974 *Phys. Rev. B* **9** 4733–41
[38] Allen P B 1972 *Phys. Rev. B* **6** 2577–9
[39] Schrieffer J R 1964 *Theory of Superconductivity* (New York: Benjamin)
[40] Allen P B and Dynes R C 1975 *Phys. Rev. B* **12** 905–22
[41] Primak W, Kaufman H and Ward R 1948 *J. Am. Chem. Soc.* **70** 2043–6
[42] Jain A *et al* 2013 *APL Mater.* **1** 011002
[43] Güntert O J and Faessler A 1956 *Z. Kristallogr.* **107** 357–61
[44] Skriver H L 1982 *Phys. Rev. Lett.* **49** 1768–72
[45] Nagara H, Mukose K, Ishikawa T, Geshi M and Suzuki N 2010 *J. of Phys.: Conference Series* **215** 012107
[46] Heyd J and Scuseria G E 2004 *J. Chem. Phys.* **121** 1187–92
[47] Heyd J, Scuseria G E and Ernzerhof M 2003 *J. Chem. Phys.* **118** 8207–15